The Astrophysical Journal Letters, 939:L10 (7pp), 2022 November 1 https://doi.org/10.3847/2041-8213/ac9839

Most Planets Might Have More than 5 Myr of Time to Form

Susanne Pfalzner[1,2], Shahrzad Dehghani[1,3], and Arnaud Michel[4]
[1] Jülich Supercomputing Center, Forschungszentrum Jülich, D-52428 Jülich, Germany; s.pfalzner@fz-juelich.de
[2] Max-Planck-Institut für Radioastronomie, Auf dem Hügel 69, D-53121 Bonn, Germany
[3] Department of Physics, University of Cologne, Cologne, Germany
[4] Department of Physics, Engineering Physics and Astronomy, Queen's University, Kingston, ON K7L 3N6, Canada
Received 2022 August 1; revised 2022 October 4; accepted 2022 October 5; published 2022 October 27

Abstract

The lifetime of protoplanetary disks is a crucial parameter for planet formation research. Observations of disk fractions in star clusters imply median disk lifetimes of 1–3 Myr. This very short disk lifetime calls for planet formation to occur extremely rapidly. We show that young, distant clusters (⩽5 Myr, >200 pc) often dominate these types of studies. Such clusters frequently suffer from limiting magnitudes leading to an over-representation of high-mass stars. As high-mass stars disperse their disks earlier, the derived disk lifetimes apply best to high-mass stars rather than low-mass stars. Including only nearby clusters (<200 pc) minimizes the effect of limiting magnitude. In this case, the median disk lifetime of low-mass stars is with 5–10 Myr, thus much longer than often claimed. The longer timescales provide planets ample time to form. How high-mass stars form planets so much faster than low-mass stars is the next grand challenge.

Unified Astronomy Thesaurus concepts: Planet formation (1241); Young star clusters (1833); Protoplanetary disks (1300); Exoplanets (498)

1. Introduction

The disks surrounding young stars provide the building material for planets. While terrestrial mantle rocks show that the Earth took tens of Myr to form (Halliday & Kleine 2006), such direct formation dating is impossible for gas giants and exoplanets. Therefore, the frequency of disks around stars of different ages is used as a method to obtain information about the time available for planet formation (Haisch & Lada 2001). The derived median disk lifetime is a "make-or-break" test for planet formation theories. As stellar ages of individual stars are intrinsically highly imprecise (e.g., Bell et al. 2013; Richert et al. 2018), disk fractions, f_d, in young star clusters are used instead. As clusters consist of fairly coeval stars, their ages can be determined with higher accuracy than for individual stars.

The decline of the disk fraction with cluster age, t, has been shown for many different disk indicators, such as infrared excess or accretion signatures (Haisch & Lada 2001; Hernández et al. 2007; Fedele et al. 2010; Ribas et al. 2014; Richert et al. 2018). Exponential fits of the form $f_d(t) = \exp(-t/\tau)$ provide an inconsistent picture with median disk lifetimes ranging from 1–3.5 to 5–10 Myr. As at least half the stars in the field seem to harbor planets (e.g., Winn & Fabrycky 2015), the shorter disk lifetimes would imply extremely rapid planet growth.

The uncertainties in cluster age determination (Bell et al. 2013) are a known problem in deducing disk lifetimes from cluster disk fractions. Additionally, environmental effects can lead to lower disk fractions in the dense cluster centers (Guarcell et al. 2007; Pfalzner et al. 2014). Also, these effects play a part; here we show that the main reason for the discrepancy in the derived disk lifetimes is its sensitivity to cluster selection regarding age and distance. We suggest that the stellar mass dependence might skew the results toward short disk lifetimes. We find that restricting the sample to nearby (<200 pc) clusters with an adequate balance between young and old clusters leads to much longer median disk lifetimes of 5–10 Myr. The disk fractions of the individual clusters in this sample are from two works (Michel et al. 2021; Luhman 2022). Within these two sources, the same method was used to determine the disk fractions.

2. Correlation between Cluster Sample and Disk Lifetime

The work by Haisch & Lada (2001) held the promise that additional data would lead to a well-defined decline of the disk fraction with cluster age. However, the more data became available, the wider the spread became. This spread is often interpreted as being caused by external disk dispersal mechanisms. While this explains the lower disk fraction in dense clusters (typical $n \approx 10^4$ pc^{-3}, Gutermuth et al. 2005; see clusters indicated in green in Figure 1, top left, Stolte et al. 2015; Vincke & Pfalzner 2018; Concha-Ramirez et al. 2021), it fails to account for the higher disk fractions in sparse clusters (typical $n < 0.5$ pc^{-3}). The black curve in Figure 1 is based on clusters with $n < 600$ pc^{-3}, where the effect of close stellar flybys on the disk fractions is restricted to small areas close to the cluster center. Many of them have no O stars or much few than Upper Sco or UCL/LCC, excluding external photoevaporation as the main cause for the difference in disk fraction. In total the environmental effect on the disk fraction should be small (<5%; Vincke & Pfalzner 2018; Concha-Ramirez et al. 2021) in these clusters. Furthermore, the disk fractions of older sparse associations and comoving groups are up to 25% higher (Figure 1, top right, red data points) higher than for the black curve. Thus density effects cannot be dominantly responsible for this large difference.

Most clusters are detected as overdensity relative to the background and elevated infrared excesses. Young clusters are identifiable even if they contain only a few hundreds or even tens of stars. When young clusters lose most of their gas

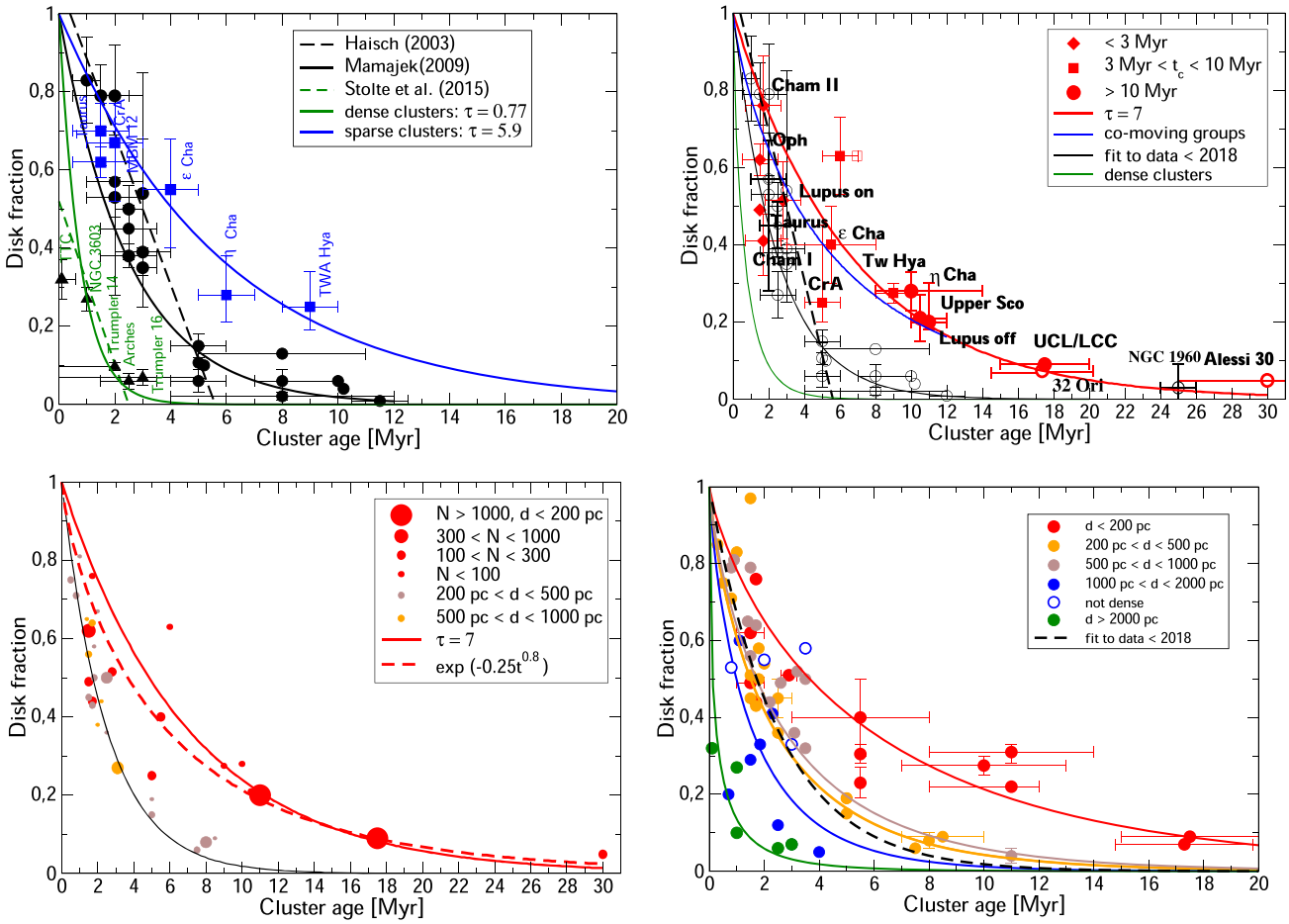

Figure 1. Disk fraction vs. cluster age. Top left: distinction between areas of different density. Clusters generally used are shown in black, compact, dense clusters in green, and sparse clusters in blue. The original fit by Haisch (dashed black line). Top right: fit using only clusters within 200 pc with the age range 1–20 Myr equitably covered (red line and symbols). Bottom left: clusters within 1000 pc. Symbols area proportional to the number of stars considered and the color representing the cluster distance. Bottom right: disk fractions color-coded according to cluster distance.

Table 1
Examples of the Fraction of Old and Nearby Clusters in Disk Lifetime Studies

References	Number of Clusters	Fraction of Clusters with		Disk Lifetime
		$t_c \geqslant 5$ Myr	$d \leqslant 200$ pc	
Richert et al. (2018)	69	0.00	0.00	1.3–3.5
Haisch & Lada (2001)	7	0.15	0.28	3.0
Hernández et al. (2008)	18	0.17	0.22	<5
Fedele et al. (2010)	10	0.20	0.33	2.9
Briceño et al. (2019)	9	0.55	0.00	2
Ribas et al. (2014)	22	0.15	0.54	2
Ribas et al. (2015)	11	0.5	0.73	5.2
Michel et al. (2021)	11	0.36	0.91	8.0
This work, Figure 1 (top right)	14	0.50	1.0	7–8

content at the end of the star formation phase (e.g., Lada & Lada 2003; Kuhn et al. 2019), their size increases to 5–10 times its initial value at ages 1–5 Myr. Thus, older clusters must contain $N > 1000$ stars to be detectable. This is why low-N clusters older than 5 Myr are missing from plots like Figure 1 (top right). Exceptions are the comoving groups, as they are discovered as moving in the same phase space independent of their surface density.

Due to their initial compactness, clusters are identifiable at much larger distances at young ages than later. Table 1 shows that studies including a significant fraction of distant clusters arrive at shorter median disk lifetimes. Even studies that include many old clusters, but all at large distances, show this trend. Our central hypothesis is that limiting magnitude at large distances introduces a bias toward brighter high-mass stars. As high-mass stars tend to lose their disks earlier (see, e.g., Carpenter et al. 2006; Ribas et al. 2015), this skews the resulting disk lifetimes toward shorter values.

Most young clusters contain 10–1000 times fewer stars than the older clusters (Pfalzner et al. 2014). This makes the individual disk fraction of young clusters less statistically significant in deriving the disk lifetime than these of older

clusters. In many studies, young clusters are overrepresented, while older clusters are underrepresented. For example, in Haisch & Lada (2001) about 85% of clusters and all 69 clusters in Richert et al. (2018) were $\leqslant$5 Myr. Table 1 shows examples of the fraction of clusters >5 Myr in various studies. Studies with large fractions of young clusters tend to derive shorter median disk lifetimes (<5 Myr) than those with more long-lived clusters (>5 Myr).

3. Median Disk Lifetimes

To avoid these biases, we include nearby clusters (<200 pc) with an equitable weight over the entire age range 1–20 Myr. Our sample contains four clusters aged 1–3 Myr, five aged 3–8 Myr, and four aged 8–20 Myr. Figure 1 (top right) shows that the resulting decline of disk fraction with cluster age (red solid line) is shallower than in studies mainly based on young distant clusters (black line; for values see Table 2). We fitted different types of curves to the data. We find that the dependence of the disk fraction on cluster age can be approximated by a one-parameter exponential function of the form $f_D = \exp(-t/7)$ with a median disk lifetime of 5.0 Myr or a two-parameter exponential function of the form $f_D = \exp(-0.25t^{0.8})$. These fits exclude the data of the even older clusters ~25 Myr old NGC 1960 and the 25–35 Myr old Alessi 30 (Galli et al. 2021a) as it is unclear whether their disks are protoplanetary or debris in nature. As an alternative, we also performed a Gaussian fit of the corresponding disk life distribution (see the accompanying research note, Pfalzner 2022). In this case, we obtain a median disk lifetime of 6.5 ± 1.5 Myr. Independent of the applied method, the derived median disk lifetimes exceed considerably the usually quoted 1–3 Myr. We emphasize that 25% of disks exist beyond 10 Myr and ≈10% beyond 15 to 20 Myr.

The question is how statistically significant is this result. Everything else being equal, the disk fractions of high-N clusters are statistically more significant. Figure 1 (bottom left) shows the disk fraction as a function of cluster age for the clusters within 1 kpc (see Table 2). However, here the symbol area is approximately proportional to the number of stars, N, considered in determining the disk fraction. It becomes apparent that the disk fractions of Upper Sco and UCL/LCC are considerably more statistically significant than those of the younger clusters. In total, there are 448 stars surrounded by a protoplanetary disk in Upper Sco and UCL/LLC in Luhman (2022). Therefore, it is improbable that some extreme outlier stars dominate by their exceptionally long disk lifetimes. Thus the result of a median disk lifetime exceeding 5 Myr seems to be highly statistically significant.

Besides these selection effects, some older studies assumed Upper Sco was younger and had a lower disk fraction. Age estimates for Upper Sco range from 5 to 12 Myr (e.g., Preibisch et al. 2002; Pecaut & Mamajek 2016), however, with an increasing consensus toward an age of 10–12 Myr (Feiden 2016; Asensio-Torres et al. 2019). Before GAIA, significant uncertainties in membership existed, especially in the cluster outskirts. Disk fractions in the outer areas could be up to 3 times lower due to false positives at that time (Rizzuto et al. 2012). One strategy to avoid the problem of false positives was to consider only the central cluster areas. However, at least for high-mass clusters older than 3–5 Myr, this introduces a bias toward lower disk fractions caused by external disk destruction (Pfalzner et al. 2014). Nowadays, the false-positive rate in the outskirts of clusters is much lower. Recent disk fractions of Upper Sco are nearly twice as high as the 11% used in several older studies. Similarly, for the 15–20 Myr old UCL/LCC region, disk fraction values increased from 1%–3% to 9% nowadays.

Why does restricting to nearby clusters with an even spread in cluster ages lead to a longer disk lifetime? Michel et al. (2021) found the disk fraction of Upper Sco to be very similar to that of comoving groups of similar age. They argue that the low-UV radiation in both samples is the reason for the similarity in disk fractions. In the following, we reason that distance rather than similar radiation levels might lead to disk fractions being similar for these otherwise quite different environments.

4. Median Disk Lifetime: A Question of Stellar Mass

Many studies found disk fractions to be lower for high-mass than low-mass stars (e.g., Carpenter et al. 2006; Roccatagliata et al. 2011; Yasui et al. 2014; Ribas et al. 2015; Richert et al. 2018). Here we hypothesize that this stellar mass dependence of disk fractions is partly responsible for the wide spread in disk fractions at any given age. Most stars are of low mass (M- and K-type); however, observations of more distant clusters or at low sensitivity suffer from limiting magnitude. Thus mean stellar mass is higher as low-mass stars are underrepresented in these samples. This bias toward higher stellar mass affects the derived disk lifetimes directly. As high-mass stars lose their disks faster (e.g., Ribas et al. 2015), distant cluster disk fractions are systematically lower. Consequently, the derived disk lifetimes are shorter.

We test this hypothesis by plotting the disk fractions as a function of stellar age color-coded by cluster distance (Figure 1, bottom left). A strong correlation between the slope of the decline in disk fraction with cluster distance becomes apparent. Obviously, current median disk lifetimes suffer from a strong selection effect connected to cluster distance. Here cluster distance is only a crude proxy for missing out on low-mass stars in the more distant samples but is sufficient to demonstrate the problem.

The mean density of distant clusters like Arches or Trumpler 14 clusters is about 1000 times higher than in clusters like the ONC. These dense clusters are located at distances >2000 pc. Therefore, they are strongly affected by limiting magnitude. The derived very low disk fractions usually apply only to stars with masses >1 $M_\odot$. However, environmental effects should also apply to these clusters (Mann et al. 2014; Vincke & Pfalzner 2016; Ansdell et al. 2017). However, determining the relative importance of mass dependence versus environment remains a challenging task.

Upper Sco has a disk fraction of $5\%^{+4\%}_{-3\%}$ for B7–K5.5-type stars (Luhman 2022) compared to $22\% \pm 0.02$ for low-mass stars (M3.7–M6). Similarly, for the UCL/LLC, the disk fraction is $0.7\%^{+0.06}_{-0.04}$ for higher-mass stars compared to $9\% \pm 1\%$ for low-mass stars. The statistical significance of these data is quite high, even when separated into mass bins. For M3.75–M6 stars (22%) it is based on 633 objects, for K6–M3.5 stars (18%) on 311 objects, and for B7–K5.5-type stars ($5\%^{+4\%}_{-3\%}$) on 76 objects in Luhman (2022). So even for the high-mass star, the statistical sample is as large as many young low-mass clusters' total population. The statistical significance is even higher for the UCL/LLC data, with sample sizes of 2488, 725, and 452 in the equivalent stellar mass bins.

Table 2
Disk Fractions

Identification	d (pc)	Age (Myr)	$N_{\rm stars}$	f_d	Limit	Median Mass ($M_\odot$)	$\log(\rho_c)$ ($M\odot$ pc^{-3})	Source
$d \ll 200$ pc								
Alessi 30	108	30	162	0.049[a]	0.04 $M_\odot$			(a)
UCL/LLC	150	15–20	3665	0.09		0.15	−0.85 −(−1.05)	(b)
32 Ori	95	15–20	160	0.07		0.15		(f1)
Upp Sco	145	10–12	1774	0.22/0.20	0.01 $M_\odot$	0.15	−0.59	(b), (c)
Lupus-off cloud	160	10–12	60	0.21 ± 0.06	0.05 $M_\odot$			(l)
η Cha	94	8–14	40	0.28/33				(d)
TW Hya	56	7–13	56	0.25/0.30				(d)
Lupus-on cloud	160	6	30	0.63 ± 0.04	0.05 $M_\odot$			(l)
CrA	152	5	146	0.23 ± 0.4	0.04 $M_\odot$			(d)
ϵ Cha	101	5 (3–8)	90	0.5/0.3[b]				(d), (e)
Lupus	158	2.6–3.1	158	0.50/0.53	0.03 $M_\odot$			(a), (d)
Cham I	188	1.7	183	0.44	$6 < G < 20$			(f)
Cham II	197	1.7	41	0.76	G12-G18			(f)
Taurus	128–196	1–2	137	0.49	0.05 $M_\odot$			(i)
Ophiuchus	139	1–2	420	0.62				(i)
200 pc $< d <$ 500 pc								
25 Orionis	330	8.5 ± 1.5	26	0.09				(g)
Ori 1a	355	8	811	0.08	0.1 $M_\odot$		−0.54	(a1)
γ Vel	345	7.5	125	0.06	0.2 $M_\odot$			(i)
λ Ori	414	5	43	0.19				(i)
OriOB1b	414	5	278	0.15	0.04 $M_\odot$		0.55	(i)
IC 348	310	2–3	310	0.50/0.40			2.2	(d)
σ Ori	414	2.5	71	0.36		0.3 $M_\odot$		(i)
NGC 2068/NGC 2071	400	1–3	67	0.54				(j)
Berkley59	400	1.8	201	0.50	0.1 $M_\odot$	0.78		(k)
Serpens South	415	1.8	26	0.58	0.1 $M_\odot$	0.3		(k)
ONC Flank	414	1.7	236	0.43	0.13 $M_\odot$	0.52	1.3	(k)
OMC	414	1.5	181	0.45	0.09 $M_\odot$	0.32		(k)
L1630N	400	1.5		0.97				(l)
Lynds1641	400	1.5		0.51				(m)
NGC 1333	320	1.0	73	0.81				(j)
Flame/NGC 2023	414	0.8	142	0.71	0.1	0.38 $M_\odot$		(k)
Serpens	425	0.5	137	0.75				(j)
NGC 2024	415	0.3		0.85			2.424	(a1)
500 pc $< d <$ 1000 pc								
NGC 7160	900	11 ± 1	⋯	0.04 ± 0.03				(b1)
CepOB3b-East	700	3.5		0.32				(x)
CepOB3b-West	700	3.5		0.50				(y)
NGC 2264	760	3.2	324	0.52				(c1)
	751	3.1		0.38				(j)
Trumpler37	900	2.6		0.49				(j)
CepC	700	2.2	59	0.44	0.1 $M_\odot$	0.47		(k)
CepA/A	700	2.0	77	0.38	0.1 $M_\odot$	0.43		(k)
MonR2	830	1.7	208	0.64	0.09 $M_\odot$	0.47	1.72	(k)
LkH α101	510	1.5	140	0.56	0.1 $M_\odot$	0.56		(k)
L988e	700	1.5		0.79				(d1)
Continued on next page								
CepA/C	700	1.4	86	0.65	0.1 $M_\odot$	0.38		(k)
RCW36	700	0.9		0.81	0.1 $M_\odot$	0.35		(k)
W40	500	0.8		0.79	0.1 $M_\odot$	0.53		(k)
1000 pc $< d <$ 2000 pc								
NGC 6231	1585	4		0.05				(n)
NGC 2282	1650	3.5		0.58				(o)
NGC 7129	1260	3		0.33 ± 0.22				(q)
W3Main	1950	3		0.07				(r)

Table 2
(Continued)

Identification	d (pc)	Age (Myr)	N_{stars}	f_d	Limit	Median Mass ($M_\odot$)	$\log(\rho_c)$ ($M_\odot$ pc^{-3})	Source
NGC 2244	1880	3	570	0.445			1.03	(e1)
NGC 2362	1480	2.5		0.12				(k)
M8	1300	2.3		0.41				(k)
AFGL333	2000	2.0		0.55 ± 0.5				(s)
NGC 6611	1995	2.0		0.59				
	1750	1.2		0.34			1.45	(u)
Pismis 24	1700	1.85		0.33				(t)
Cyngus OB2	1450	1.5		0.29			1.61	(u)
M 17	2000	1.1	35	0.6	0.12 $M_\odot$	3.68		(k)
Sh2-106	1400	0.8	92	0.53 ± 0.1	0.13 $M_\odot$	0.6		(k)
NGC 6530	1300	0.7		0.20				(v)
$d > 2000$ pc								
Trumpler 15	2360	8.0		0.021	1 $M_\odot$			(w)
Bochum 1	2800	5.0		0.086	A–B			(w)
Quintuplett	8000	4.0	766	0.04	A–B		3.7	(z)
Trumpler 16	2700	3.0		0.069	1 $M_\odot$			(w)
Trumpler 14	2800	2.0		0.097	1 $M_\odot$		4.3	(w)
Arches	8000	2.5		0.092	A–B		5.6	(z)
NGC 3603	3600	1.0		0.27			5.0	(z)
TTC	2700	0.1		0.32	1 $M_\odot$			(w)

Notes.
[a] Possibly debris disk fraction.
[b] The disk fraction is much higher in the center than the outskirts (>10 pc) of η Cha.
References. (a) Galli et al. (2021a), (b) Luhman (2022), (c) Luhman & Esplin (2020), (d) Michel et al. (2021), (e) Dickson-Vandervelde et al. (2021), (f) Galli et al. (2021b), (g) Ribas et al. (2014), (i) Manzo-Martínez et al. (2020), (j) Sung et al. (2009), (k) Richert et al. (2018), (l) Spezzi et al. (2015), (m)Fang et al. (2013), (n) Damiani et al. (2016), (o)Dutta et al. (2015), (q) Stelzer & Scholz (2009), (r) Bik et al. (2014), (s)Jose et al. (2016), (t) Fang et al. (2012), (u) Guarcello et al. (2016), (v) Damiani et al. (2006), (w) Preibisch et al. (2011), (x) Allen et al. 2008, (y) Allen et al. (2012), (z) Stolte et al. (2015), (a1) Briceño et al. (2019), (b1) Hernández et al. (2008), (c1) Sousa et al. (2019), (d1) Allen et al. (2008), (e1) Balog et al. (2007).

This dependence of the disk fractions on stellar mass translates into shorter disk lifetimes for high-mass than low-mass stars. Figure 2 shows a simple extrapolation based on the Upper Sco and UCL/LLC data, assuming an initial disk fraction of 100%. Basing the curves on just three points is not ideal (the third one being the assumed primordial disk fraction, but as shown in Figure 1, bottom, the fit for the total disk fraction holds for additional clusters). Nevertheless, it illustrates the critical point of the mass dependence of the decline in disk fraction. Using Figure 2 as a first indication, we expect that 50% of the low-mass stars still have a disk at ≈5 Myr. By contrast, only <20% of the high-mass stars retain their disks at that age. Half of the high-mass stars have already lost their disks at ≈2 Myr. Thus the median disk lifetime of high- and low-mass stars seems to differ by at least a factor of 2.

There is considerable uncertainty of the zero-age disk frequency (Michel et al. 2021). If all stars are initially surrounded by disks, the median disk frequency for the low-mass stars would be 5–7 Myr, whereas for initial disk frequencies of 80%, the median disk lifetime increases to 6–10 Myr (see Figure 2). Here again the higher values are obtained when performing a Gaussian fit to the corresponding disk life distribution.

The mass-dependent disk lifetime could be determined from the disk fractions for the different stellar masses. Unfortunately, there is a lack of statistically meaningful data for high stellar masses. Figure 3 illustrates the general trend based on the Upper Sco and UCL/LCC data. Both scenarios (initial disk frequency of 100% and 80%) show the same overall trend: for

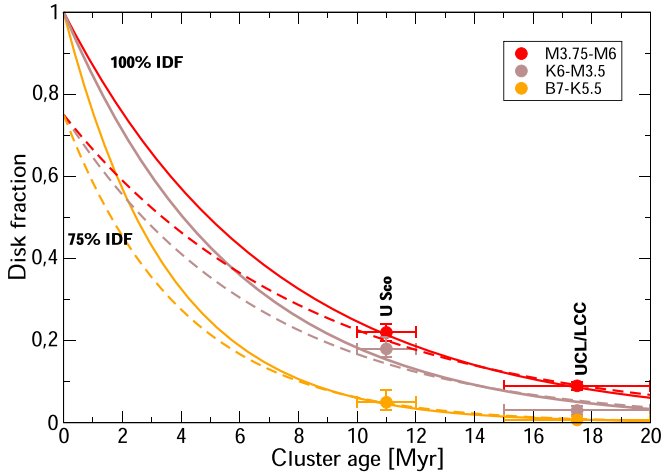

Figure 2. Disk fraction vs. cluster age. Fits for mass-dependent disk lifetimes based on the high-significance values of Upper Sco and UCL/LCC assuming an initial disk fraction of 100% (solid line) and 75% (dashed line).

M–K stars, the median disk lifetime is basically the same, but for higher-mass stars, it is considerably lower. However, where precisely the decline in disk lifetimes happens remains uncertain. This relation requires urgent further observational investigation.

Why do high-mass stars lose their disks so much earlier than low-mass stars? One answer might lie in their higher efficiency in accreting material and photoevaporation. Wilhelm &

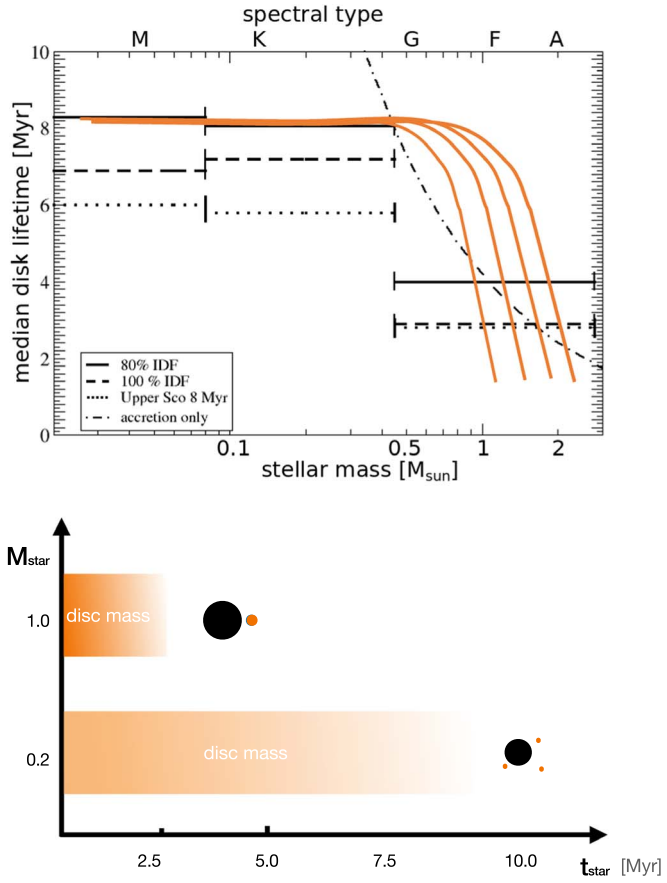

Figure 3. Top: median disk lifetime as function of stellar mass assuming 100% initial disk fraction (dashed lines), 80% initial disk fraction (solid lines), and a lower Upper Sco age of 8 Myr instead of 11 Myr (dotted lines). The orange lines show the general trend including the uncertainty for higher-mass stars. Bottom: correlation between disk lifetime and properties of planetary system.

Portegies Zwart (2022) find that stars with masses exceeding 0.8 $M_\odot$ have shorter lifetimes due to these two effects; nevertheless, lifetimes up to 15 Myr are still possible for all host star masses up to 2 $M_\odot$. The critical role of accretion is supported by observations finding that the lowest M stars that still retain a disk at ages ≈8–10 Myr also show moderate accretion levels (Venuti et al. 2019).

5. From the Diversity of Disk Lifetimes to That of Planets

The biggest surprise in exoplanet observations is the immense diversity in planets and planetary systems (Howard 2013; Gaudi et al. 2021). Suggested causes are, among others, differences in the disk mass and disk mass profile (Kokubo & Ida 2002), the metallicity of the stars (Petigura et al. 2018), the location of rings in disks (van der Marel & Mulders 2021), and the type of cluster environment (Bate 2018; Vincke & Pfalzner 2018; Winter et al. 2020).

The variation in individual disk lifetime has also been suggested to influence the type of planet that forms and the architecture of the planetary systems (Carpenter et al. 2005; Luhman & Mamajek 2012; Ribas et al. 2015). If that holds, the stellar mass dependence of the disk lifetime should result in differences in the planets as a function of stellar mass.

Disk masses scale quasi-linearly with stellar mass (e.g., Andrews 2020). Thus high-mass stars have a much larger gas and dust reservoir for planet formation. Therefore, it is not surprising that main-sequence FGK stars host more larger planets than low-mass stars (Howard et al. 2012; Sabotta et al. 2021). However, the situation is different for smaller planets. M dwarfs host about a factor of 3 more small planets (1.0–2.8 $R_\oplus$) than main-sequence FGK stars (e.g., Mulders et al. 2021). However, the mass is not simply redistributed into more smaller planets. Surprisingly, the average heavy-element mass decreases with increasing stellar mass from 7 $M_\oplus$ for M stars to 5 $M_\oplus$ for G and K stars and 4 $M_\oplus$ for F stars. Thus despite M star disks containing 10 times less mass, they are nearly 20 times more efficient than F stars in converting the disk's heavy-element content into planetary material. The higher heavy-element content also corresponds to a higher fraction of stars with planetary systems for low-mass stars (Yang et al. 2020; He et al. 2021).

The strong dependence of the disk lifetime on stellar mass may explain the high planet formation efficiency in low-mass stars. High-mass stars seem to produce their high-mass gas giants on timescales shorter than 3 Myr while failing to form additional low-mass planets. By contrast, low-mass stars form large planets to a lower degree; however, their long disk lifetimes allow for the formation of many small planets. In a way, slow but steady beats fast and short.

Forming low-mass planets on timescales >5 Myr lowers the hurdles for the standard accretion model. However, explaining why high-mass stars form more massive planets on considerably shorter timescales remains a significant challenge. A possible explanation is that their higher disk masses make their disks more prone to gravitational instabilities. However, as $M_d/M_s \sim$ const is independent of stellar mass, the parameter Q that describes the stability of disks should be the same for high- and low-mass stars. Therefore, unstable disks are at least not a straightforward explanation. Thus, the reason for fast planet formation around high-mass stars remains an open question.

6. Summary and Conclusion

We investigated the role of cluster sample selection on derived median disk lifetimes. We find that samples with a large fraction of distant, young clusters (>200 pc; <5 Myr) tend to derive short disk lifetimes (1–3 Myr). Samples including higher fractions of nearby, older clusters arrive at higher disk lifetimes (>5 Myr). Restricting to clusters closer than 200 pc aged between 1 and 20 Myr, we obtain a median disk lifetime of 5–10 Myr.

One main reason for this discrepancy is that distant clusters are affected by limiting magnitude. Therefore, the disk fraction of, on average, higher-mass stars is determined in distant clusters. As the disk lifetime of high-mass stars is shorter than for low-mass stars, the disk fractions of more distant clusters seem lower due to this selection effect. We conclude that disk lifetimes derived from samples including many distant clusters (>200 pc) represent mostly high-mass stars. Indeed, if we only consider the high-mass stars in the sample limited to distances <200 pc, we recover a disk lifetime of only 2–4 Myr.

However, these disk lifetimes are not representative of most of the stars. Low-mass stars have a median disk lifetime of 5–10 Myr. The actual value depends mainly on the assumed initial disk fraction. If all stars are surrounded by disks at cluster ages $t_c = 0$ Myr, the median disk lifetime is 5–6 Myr. However, some stars seem to be born diskless or lose their disk extremely rapidly to planet formation. An initial disk fraction

of 70%–80% would increase the disk dissipation times for low-mass stars to 8–10 Myr and that of high-mass stars to 4–5 Myr.

For low-mass stars, the median disk lifetime of 5–10 Myr significantly relaxes the temporal constraints on planet formation. These long disk lifetimes allow for sufficient time for planets to form via accretion. The diversity of disk lifetimes might influence the structure of the emerging planetary system. It could be responsible for low-mass stars having considerably higher efficiency in using the heavy-element content in their disk for planet formation. Despite having considerably lower disk masses to start with, these low-mass stars produce a larger number of lower-mass planets. The real challenge remains to explain how high-mass stars can form planets on such a short timescale.

Currently, the effect of the environment on the disk lifetime is still not quantifiable. Only disk fractions for high-mass star clusters have been determined for dense clusters due to their general large distances (>2000 pc). A comparison is difficult even for those high-mass stars as the initial disk fraction in these dense clusters is unknown. Its uncertainty is very high, as none of the measured disk fractions exceed 32%.

Generally, determining the initial disk fraction is the next step to determine disk lifetimes accurately. This includes potential dependencies on stellar mass, cluster density, and binarity.

We thank the referee for the constructive report and useful suggestions that significantly improved our manuscript. We would like to thank K. Luhman for helpful advice on interpreting his results on the disk fractions in Upper Sco and UCL/LCC.

ORCID iDs

Susanne Pfalzner https://orcid.org/0000-0002-5003-4714
Arnaud Michel https://orcid.org/0000-0003-4099-9026

References

Allen, T. S., Gutermuth, R. A., Kryukova, E., et al. 2012, ApJ, 750, 125
Allen, T. S., Pipher, J. L., Gutermuth, R. A., et al. 2008, ApJ, 675, 491
Andrews, S. M. 2020, ARA&A, 58, 483
Ansdell, M., Williams, J. P., Manara, C. F., et al. 2017, AJ, 153, 240
Asensio-Torres, R., Currie, T., Janson, M., et al. 2019, A&A, 622, A42
Balog, Z., Muzerolle, J., Rieke, G. H., et al. 2007, ApJ, 660, 1532
Bate, M. R. 2018, MNRAS, 475, 5618
Bell, C. P. M., Naylor, T., Mayne, N. J., Jeffries, R. D., & Littlefair, S. P. 2013, MNRAS, 434, 806
Bik, A., Stolte, A., Gennaro, M., et al. 2014, A&A, 561, A12
Briceño, C., Calvet, N., Hernández, J., et al. 2019, AJ, 157, 85
Carpenter, J. M., Mamajek, E. E., Hillenbrand, L. A., & Meyer, M. R. 2006, ApJL, 651, L49
Carpenter, J. M., Wolf, S., Schreyer, K., Launhardt, R., & Henning, T. 2005, AJ, 129, 1049
Concha-Ramírez, F., Wilhelm, M. J. C., Zwart, S. P., van Terwisga, S. E., & Hacar, A. 2021, MNRAS, 501, 1782
Damiani, F., Micela, G., & Sciortino, S. 2016, A&A, 596, A82
Damiani, F., Prisinzano, L., Micela, G., & Sciortino, S. 2006, A&A, 459, 477
Dickson-Vandervelde, D. A., Wilson, E. C., & Kastner, J. H. 2021, AJ, 161, 87
Dutta, S., Mondal, S., Jose, J., et al. 2015, MNRAS, 454, 3597
Fang, M., van Boekel, R., Bouwman, J., et al. 2013, A&A, 549, A15
Fang, M., van Boekel, R., King, R. R., et al. 2012, A&A, 539, A119
Fedele, D., van den Ancker, M. E., Henning, T., Jayawardhana, R., & Oliveira, J. M. 2010, A&A, 510, A72
Feiden, G. A. 2016, A&A, 593, A99
Galli, P. A. B., Bouy, H., Olivares, J., et al. 2021a, A&A, 654, A122
Galli, P. A. B., Bouy, H., Olivares, J., et al. 2021b, A&A, 646, A46
Gaudi, B. S., Meyer, M., & Christiansen, J. 2021, in ExoFrontiers; Big Questions in Exoplanetary Science, ed. N. Madhusudhan (Bristol: Institute of Physics Publishing), 2
Guarcell, M. G., Prisinzano, L., Micela, G., et al. 2007, A&A, 462, 245
Guarcello, M. G., Drake, J. J., Wright, N. J., et al. 2016, arXiv:1605.01773
Gutermuth, R. A., Megeath, S. T., Pipher, J. L., et al. 2005, ApJ, 632, 397
Haisch, K. E. J., Lada, E. A., & Lada, C. J. 2001, ApJL, 553, L153
Halliday, A. N., & Kleine, T. 2006, in Meteorites and the Timing, Mechanisms, and Conditions of Terrestrial Planet Accretion and Early Differentiation, ed. D. S. Lauretta & H. Y. McSween (Tucson, AZ: Univ. Arizona Press), 775
He, M. Y., Ford, E. B., & Ragozzine, D. 2021, AJ, 162, 216
Hernández, J., Hartmann, L., Calvet, N., et al. 2008, ApJ, 686, 1195
Hernández, J., Hartmann, L., Megeath, T., et al. 2007, ApJ, 662, 1067
Howard, A. W. 2013, Sci, 340, 572
Howard, A. W., Marcy, G. W., Bryson, S. T., et al. 2012, ApJS, 201, 15
Jose, J., Kim, J. S., Herczeg, G. J., et al. 2016, ApJ, 822, 49
Kokubo, E., & Ida, S. 2002, ApJ, 581, 666
Kuhn, M. A., Hillenbrand, L. A., Sills, A., Feigelson, E. D., & Getman, K. V. 2019, ApJ, 870, 32
Lada, C. J., & Lada, E. A. 2003, ARA&A, 41, 57
Luhman, K. L. 2022, AJ, 163, 25
Luhman, K. L., & Esplin, T. L. 2020, AJ, 160, 44
Luhman, K. L., & Mamajek, E. E. 2012, ApJ, 758, 31
Mann, R. K., Di Francesco, J., Johnstone, D., et al. 2014, ApJ, 784, 82
Manzo-Martínez, E., Calvet, N., Hernández, J., et al. 2020, ApJ, 893, 56
Michel, A., van der Marel, N., & Matthews, B. C. 2021, ApJ, 921, 72
Mulders, G. D., Drkazkowska, J., van der Marel, N., Ciesla, F. J., & Pascucci, I. 2021, ApJL, 920, L1
Pecaut, M. J., & Mamajek, E. E. 2016, MNRAS, 461, 794
Petigura, E. A., Marcy, G. W., Winn, J. N., et al. 2018, AJ, 155, 89
Pfalzner, S. 2022, arXiv:2210.11764
Pfalzner, S., Steinhausen, M., & Menten, K. 2014, ApJL, 793, L34
Preibisch, T., Brown, A. G. A., Bridges, T., Guenther, E., & Zinnecker, H. 2002, AJ, 124, 404
Preibisch, T., Ratzka, T., Kuderna, B., et al. 2011, A&A, 530, A34
Ribas, Á., Bouy, H., & Merín, B. 2015, A&A, 576, A52
Ribas, Á., Merín, B., Bouy, H., & Maud, L. T. 2014, A&A, 561, A54
Richert, A. J. W., Getman, K. V., Feigelson, E. D., et al. 2018, MNRAS, 477, 5191
Rizzuto, A. C., Ireland, M. J., & Zucker, D. B. 2012, MNRAS, 421, L97
Roccatagliata, V., Bouwman, J., Henning, T., et al. 2011, ApJ, 733, 113
Sabotta, S., Schlecker, M., Chaturvedi, P., et al. 2021, A&A, 653, A114
Sousa, A. P., Alencar, S. H. P., Rebull, L. M., et al. 2019, A&A, 629, A67
Spezzi, L., Petr-Gotzens, M. G., Alcalá, J. M., et al. 2015, A&A, 581, A140
Stelzer, B., & Scholz, A. 2009, A&A, 507, 227
Stolte, A., Hußmann, B., Olczak, C., et al. 2015, A&A, 578, A4
Sung, H., Stauffer, J. R., & Bessell, M. S. 2009, AJ, 138, 1116
van der Marel, N., & Mulders, G. D. 2021, AJ, 162, 28
Venuti, L., Stelzer, B., Alcalá, J. M., et al. 2019, A&A, 632, A46
Vincke, K., & Pfalzner, S. 2016, ApJ, 828, 48
Vincke, K., & Pfalzner, S. 2018, ApJ, 868, 1
Wilhelm, M. J. C., & Portegies Zwart, S. 2022, MNRAS, 509, 44
Winn, J. N., & Fabrycky, D. C. 2015, ARA&A, 53, 409
Winter, A. J., Kruijssen, J. M. D., Chevance, M., Keller, B. W., & Longmore, S. N. 2020, MNRAS, 491, 903
Yang, J.-Y., Xie, J.-W., & Zhou, J.-L. 2020, AJ, 159, 164
Yasui, C., Kobayashi, N., Tokunaga, A. T., & Saito, M. 2014, MNRAS, 442, 2543